

New optical structure near the E_1 transitions of InSb/InAlSb quantum wells

F. Cerdeira,* A. Pinczuk, T. H. Chiu, and W. T. Tsang

AT&T Bell Laboratories, Murray Hill, New Jersey 07974

(Received 16 April 1985)

We use resonant Raman scattering to probe into the electronic structure of InSb/InAlSb strained layer superlattices in the region of the E_1 optical gap. A new resonant enhancement peak, not present in bulk InSb, appears in narrow quantum-well samples at low temperatures. Its dependence of quantum-well width and temperature indicates the existence of another critical point in the combined density of states that becomes observable through excitonic interactions under extreme confinement of the electronic states. A similar structure is observed in GaSb/GaAlSb quantum wells. This suggests the presence of two critical points along the Λ direction of the Brillouin zone in the bulk semiconductors of this family.

The formation of quantum states or subbands in superlattices and multiple quantum wells of III-V semiconductors has been amply documented.^{1,2} Most of this research, however, concerns the subband structure of direct band-gap materials in the vicinity of the Brillouin zone center. The more general issue regarding the effect of the superlattice potential on electronic states and optical transitions at other critical points remains largely unexplored. Recent results of electroreflectance^{3,4} and resonant Raman scattering⁵ suggest that subbands also form in the region of the E_1 and $E_1 + \Delta_1$ optical gaps. The question as to how exactly the E_1 transitions are affected by the superlattice potential, however, is still unclear. In fact, the nature of the E_1 optical transitions in bulk materials has been the subject of considerable controversy.⁶⁻⁸ It is not clear whether the structure observed in the optical constants is due to direct transitions along the Λ direction extending through a large portion of the Brillouin zone, or if it comes from a critical point localized at the L point.⁸ The existence of a second, weaker, M_0 singularity close to a much stronger M_1 critical point is inferred from thermally modulated reflectance.⁷

In the present work we investigate the region of the E_1 transition in InSb/InAlSb strained layer superlattices, using resonant Raman scattering to probe into the optical interband transitions occurring in this spectral range. This technique is particularly adequate to study electronic states in superlattices and multiple quantum wells because it exploits the modulation produced in these states by the longitudinal-optical (LO) lattice vibrations characteristic of each type of layer. This selectivity as to the type of layer being probed makes it ideal to determine whether the electronic states under study are confined within the quantum wells of the smaller band-gap material or if they extend across the interface.^{9,10} In particular, the Raman cross section of the LO phonon in the Fröhlich-induced forbidden configuration has a *single* peak in the vicinity of critical points due to vertical electronic transitions.¹¹ The shape and interpretation of this resonance in bulk InSb is well understood.¹¹⁻¹⁴ In our experiments with narrow InSb quantum wells, the Raman cross section of the forbidden LO phonon at low temperatures ($T \leq 150$ K) exhibits *two* well defined peaks in the laser frequency range $1.85 \leq \hbar\omega_L \leq 2.15$ eV. The peak at higher energies evolves continuously towards the single peak found in bulk InSb (Refs. 12-14) as the width of the quantum well, d , increases. The second peak vanishes as d or T increase. The absence of any enhancement in the LO phonons originating in the alloy layers indi-

cate that the electronic transitions involved in these resonances are confined within the InSb quantum wells. A similar structure is observed in GaSb/AlGaSb quantum-well heterostructures. We propose that the extra peak in the resonant Raman cross section of narrow quantum wells reveals the existence of two critical points in the combined density of states for E_1 optical transitions (separated by ~ 100 - 150 meV). These critical points occur along the Λ direction of the Brillouin zone of the bulk, and can only be resolved by confining the electronic states within narrow quantum-well layers.

The samples used in our experiments were superlattices of InSb/In_{0.7}Al_{0.3}Sb heterostructures. A 1- μ m layer of In_{1-x}Al_xSb, graded up to $x \approx 0.2$ was first grown on a (100)InSb substrate. Subsequently, alternating layers of InSb and In_{0.7}Al_{0.3}Sb, of thicknesses d and d_0 , respectively, were grown with 15 or 30 repetitions. The end layer of all our samples consisted of 60 Å of In_{0.7}Al_{0.3}Sb. Table I lists the main parameters of our samples. The lattice mismatch between the InSb and In_{0.7}Al_{0.3}Sb is accommodated by a homogeneous tetragonal compression (extension) of the InSb (alloy) layer. The strain present in the InSb layers was determined by measuring the difference in frequency between the LO phonon in the superlattice and that in bulk (substrate) material.¹⁵ The measured values of strain ϵ in each sample are also listed in Table I. The width of the Raman line at $T=2$ K was monitored to detect the possible presence of inhomogeneous strain in the layers.^{15,16} No significant inhomogeneities in the strain distributions could be observed by this method in any of the samples listed in Table I. One sample of GaSb/GaAlSb (No. 5 in Table I) was also measured. It was grown directly on a (100)GaSb substrate, so that the GaSb layers are unstrained. The Raman measurements were performed in the backscattering configuration $z(xx)\bar{z}$, where x , y , and z coincide with the cubic axis and z is perpendicular to the layers. We used the continuous emission of a cw-dye laser with DCM, rhodamine 6G, and coumarin 6 dyes, covering the spectral region $1.85 \leq \hbar\omega_L \leq 2.30$ eV.

The Raman spectrum of the InSb/InAlSb samples consists of longitudinal-optical vibrations of the InSb (LO) and the InAlSb (LO₁) layers. A typical spectrum is shown in the inset of Fig. 1. While the cross section of the LO₁ peak remained approximately constant, that of the LO peak showed a marked dependence on incident laser frequency in the region under study (1.85-2.15 eV). This dependence, for sample No. 2 of Table I, is displayed in Fig. 1 for several

TABLE I. Main characteristics of the strained-layer superlattice samples used in our experiment. Percentual strain, $10^2\epsilon$, in the InSb sample is indicated.

Sample No.	Type	Substrate	Graded layer ($x \sim 0.2$)	x	Layer thickness (\AA)		Number of periods	$10^2\epsilon$
					d (host)	d_0 (alloy)		
1	InSb/ $\text{In}_{1-x}\text{Al}_x\text{Sb}$	InSb (100)	Yes	0.3	40	40	30	1.04
2	InSb/ $\text{In}_{1-x}\text{Al}_x\text{Sb}$	InSb	Yes	0.3	60	60	30	1.04
3	InSb/ $\text{In}_{1-x}\text{Al}_x\text{Sb}$	InSb	Yes	0.3	120	120	30	0.78
4	InSb/ $\text{In}_{1-x}\text{Al}_x\text{Sb}$	InSb	Yes	0.3	300	300	15	0.70
5	GaS/ $\text{Ga}_{1-x}\text{Al}_x\text{Sb}$	GaSb (100)	No	0.4	90	150	30	0

temperature values. At $T=10$ K the Raman cross section of the LO peak shows *two* sharp maxima located at $\hbar\omega_L = E_R(1) = 2.088$ eV and $\hbar\omega_L = E_R(2) = 1.972$ eV, respectively. The latter decreases in relative intensity as temperature increases and is not observed at room temperature. The energy of both peaks decreases as temperature increases at rates [-5.1×10^{-4} eV/K for $E_R(1)$ and -6.0×10^{-4} eV/K for $E_R(2)$] consistent with values quoted in the literature⁸ for the E_1 optical gap of InSb. The temperature dependence of the intensity of the $E_R(2)$ (lower energy) peak signals to the strong excitonic character of the optical transition involved in this resonance. The absence of any resonance enhancement in the LO_1 peak throughout the whole region indicates that the electronic states involved in

this resonance are localized within the InSb quantum wells. The same is true for all the samples examined at all temperatures.

Next we investigated the dependence of these two resonant enhancement peaks as a function of quantum well width. In Fig. 2 we show the results for the forbidden LO phonon of InSb at $T=10$ K in InSb/ $\text{In}_{0.7}\text{Al}_{0.3}\text{Sb}$ superlattices of different layer thicknesses. An arrow indicates the position of the single peak found in bulk (substrate material) InSb. A similar peak $E_R(1)$ is observed in all the superlattice samples, shifted towards higher energies by the combined effect of stress and confinement. The lower energy

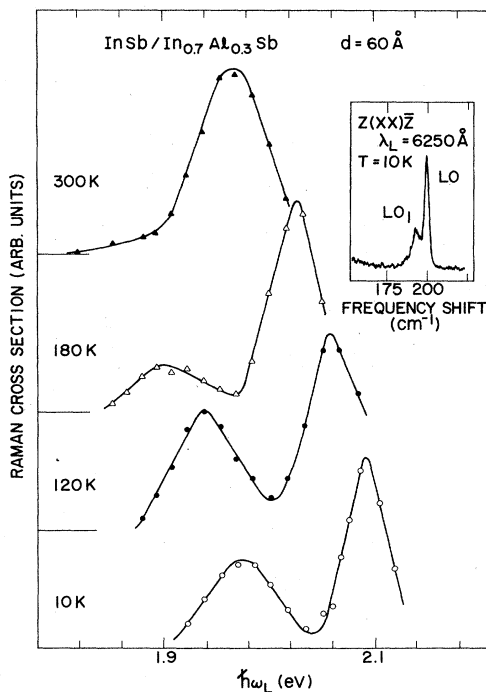


FIG. 1. Raman cross section vs incident laser frequency for the forbidden LO phonon of InSb, from sample No. 2 of Table I. A typical Raman spectrum is shown in the inset.

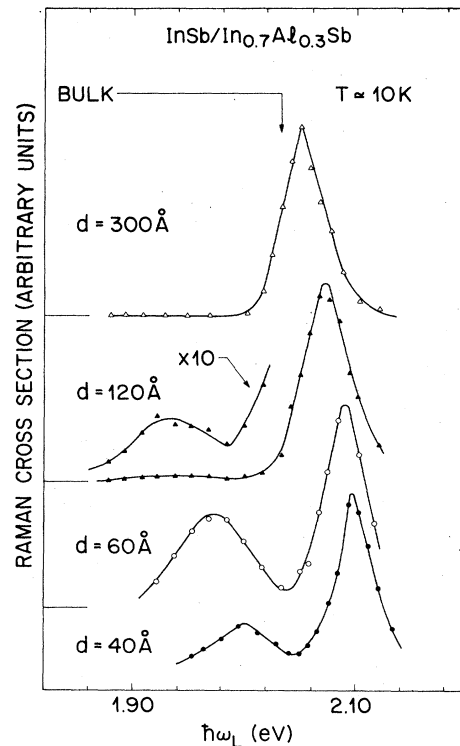


FIG. 2. Raman cross section vs incident laser frequency of the forbidden LO phonon of InSb for InSb/ InAlSb superlattices with different quantum well width (d).

peak $E_R(2)$ appears only in the samples with narrower quantum wells, being absent in bulk InSb as well as in the superlattice with $d=300$ Å (Fig. 2). This peak appears to vanish continuously as the width of the quantum well, d , increases. It shows maximum intensity [relative to the $E_R(1)$ peak] for the sample with $d=60$ Å. The dependence of the intensity of the $E_R(2)$ peak with both d and temperature signals to excitonic effects, which are stronger when both the electron and the hole are confined within a distance of the order of the excitonic radius.

Figure 2 shows that both resonant peaks move towards higher energies as the width of the quantum well decreases, although the lower energy peak $E_R(2)$ does so at a higher rate. In order to give quantitative interpretation to these data we must attempt an assignment of the optical transitions involved in each one of the resonant maxima. The higher energy peak $E_R(1)$ evolves continuously, as d increases, into the single peak observed in bulk InSb. Hence, we assign this structure to the E_1 optical gap of bulk InSb shifted towards higher energies in the superlattice by the combined effects of strain and confinement. The second peak could be assigned to another critical point in the same region ($\Lambda-L$) of the Brillouin zone, but with much weaker oscillator strength, so that it only becomes noticeable at low temperatures and under conditions of extreme confinement. The fact that the values of dE_R/dT found in this experiment are consistent with those reported in the literature for the E_1 gap,⁸ and furthermore the fact that $|dE_R(2)/dT| > |dE_R(1)/dT|$ supports this assignment.⁷ Alternatively, the $E_R(2)$ peak can be interpreted in terms of a second critical point in this energy region which occurs only in superlattice samples as a consequence of Brillouin-zone folding.² In what follows we examine our experimental results in the light of these two possible assignments.

If both resonant peaks observed in superlattice samples are related to optical transitions in bulk InSb, their energies in each type of sample (E_R and E_R^B , respectively) are related to each other as

$$E_R(\epsilon, d) = E_R^B + \Delta_s(\epsilon) + \Delta_c(d) \quad (1)$$

where Δ_s and Δ_c are energy shifts produced by strain and confinement, respectively. The former can be calculated using the data in Table I and the results of modulated reflectance in InSb under uniaxial strain,¹⁷ as

$$\Delta_s(\epsilon) = 3.016\epsilon \quad (\Delta_s \text{ in eV}) \quad (2)$$

The third term in Eq. (1) is more difficult to calculate. Even in the square-well model it depends on the mismatch of valence and conduction bands between both types of layers at the critical point responsible for the observed resonance. If that mismatch were very large, Δ_c could be approximated by the lowest level of a particle of mass μ^* (reduced optical mass) in an infinite square well of width d :

$$\Delta_c(d) = \frac{\pi^2 \hbar^2}{2\mu^* d^2} \quad (3)$$

Given the small difference in the E_1 gaps of InSb and $\text{In}_{0.7}\text{Al}_{0.3}\text{Sb}$ ($\Delta E_1 \sim 0.16$ eV) this approximation is not really justified. Still, we might expect Δ_c to scale approximately as d^{-2} . In Fig. 3 we plot $\bar{E}_R = E_R(\epsilon, d) - \Delta_s(\epsilon)$ vs d^{-2} and

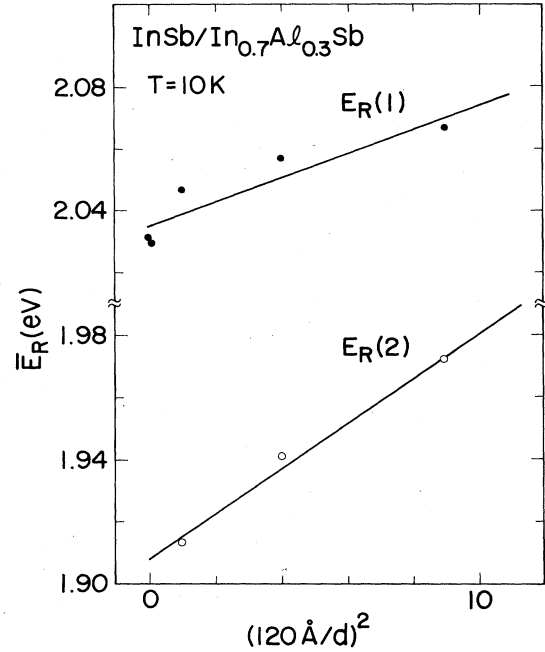


FIG. 3. Position of the resonant maxima [corrected for strain as indicated in Eqs. (1) and (2)] vs d^{-2} .

find that both peaks exhibit a fairly linear behavior, extrapolating for $d \rightarrow \infty$ to bulk values of $E_R^B(1) = 2.035$ eV and $E_R^B(2) = 1.908$ eV. The difference in slope would point to a relation between reduced optical masses of $\mu^*(1)/\mu^*(2) \approx 1.9$. Thus, our second critical point would be located at ~ 0.13 eV below the stronger singularity and be characterized by a smaller (almost half) reduced optical mass.

The alternative explanation of the low-energy peaks of Figs. 1 and 2 consists of postulating the existence of a critical point in this energy region which is absent in the bulk, but appears as a consequence of the superlattice potential in the layered samples. This would occur through zone folding along the (001) direction of the Brillouin zone.² An examination of existing band calculations¹⁸ for InSb suggests transitions from the valence band at or near the X point to the conduction band at Γ as likely candidates for the extra critical point. The small conduction-band mass would account for the bigger slope in $E_R(2)$ shown in Fig. 3, and the gradual disappearance of the additional peak as d increases. On the negative side, we would expect the folded states to extend throughout the whole superlattice, rather than be confined in the InSb layers. Also, it is rather surprising to find such a large optical matrix element for samples of large period such as $L = 2d = 120$ Å. We would also expect the relative intensity of this extra peak to continue increasing as L decreases, in contrast with the results shown in Fig. 2 for $d = 60$ and 40 Å.

There is a substantial difference between the two interpretations discussed above. The first one would imply the existence of a similar effect in other superlattices composed of zinc blende or diamond-type semiconductors, since the existence of one or two critical points in the region of the E_1 gap is likely to be a characteristic common to all materials of this family. The second explanation, transitions between

folded states, depends upon the fortuitous coincidence of the $X \rightarrow \Gamma$ transition with the E_1 optical gap. Even if this were true for InSb, it is unlikely that the same effect should be observed in superlattices made up of different III-V materials. Following this reasoning we performed the same experiment in a GaAs/GaAlSb superlattice (sample No. 5 in Table I). Although resonant Raman results in this type of superlattice were already reported,⁵ the laser frequency region studied in this previous experiment was not wide enough to find additional structure in the vicinity of the E_1 main resonance. Our results (Fig. 4) show a second resonant enhancement peak at lower energies with characteristics analogous (confined to the GaSb LO, ~ 150 meV towards lower energies, etc.) to those found in the InSb superlattices. Since the GaSb layers are unstrained, this additional structure cannot be explained away as a strain effect or be related to the particular characteristics of sample preparation. Its presence in both types of superlattice also favors the interpretation in terms of the complex nature of the E_1 singularity in this family of materials, that is brought to light by the effects of confinement of the electronic states into narrow quantum wells. It is clear that further theoretical work into the band structure of these materials, in particular, as to how it is affected by the presence of the superlattice potential, is necessary to fully understand the implications of the results presented here.

In summary, resonant Raman experiments performed in InSb/InAlSb and GaSb/GaAlSb superlattices reveal the existence of a second set of direct interband transitions in the region of the E_1 optical gap. In our opinion, the most likely explanation of this new structure, which is not present in bulk samples, is the existence of a second, but weaker, singular point in the same region of k space whose effect becomes observable through excitonic interaction when the electrons and holes are confined within a distance comparable to the excitonic radius.

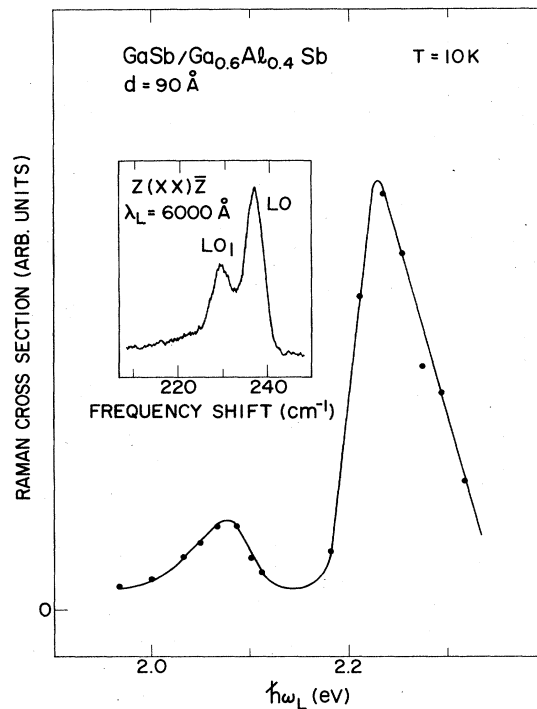


FIG. 4. Raman cross section vs incident laser frequency for the forbidden LO phonon of GaSb in a GaSb/GaAlSb superlattice. The inset shows a typical Raman spectrum of this sample.

Helpful discussions with J. C. Phillips, M. Schlüter, and P. A. Wolff are gratefully acknowledged. We thank M. G. Lamont for expert technical assistance.

*On leave from the Instituto de Física, UNICAMP, 13.100 Campinas Sao Paulo, Brazil.

¹R. Dingle, in *Festkörperprobleme*, Advances in Solid State Physics, Vol. XV, edited by H. J. Queisser (Pergamon/Viewig, Braunschweig, 1975), p. 21.

²L. Esaki, *J. Phys. (Paris) Colloq.* **45**, C5-3 (1984).

³E. E. Mendez, L. L. Chang, G. Landgren, R. Ludeke, L. Esaki, and F. H. Pollak, *Phys. Rev. Lett.* **46**, 1230 (1981).

⁴E. E. Mendez, C. A. Chang, H. Takaoka, L. L. Chang, and L. Esaki, *J. Vac. Sci. Technol. B* **1**, 152 (1983).

⁵C. Tejedor, J. M. Calleja, F. Meseguer, E. E. Mendez, C. A. Chang, and L. Esaki, in *Proceedings of the 17th International Conference on the Physics of Semiconductors*, edited by J. D. Chadi and W. A. Harrison (Springer, Heidelberg, 1985), p. 559.

⁶J. C. Phillips, in *Solid State Physics*, edited by F. Seitz and D. Turnbull (Academic, New York, 1966), Vol. 18, p. 55.

⁷F. R. Kessler and K. Dettmer, *Phys. Status Solidi (b)* **51**, 79 (1972).

⁸L. Logothetidis, L. Viña, and M. Cardona, *Phys. Rev. B* **31**, 947 (1985).

⁹J. E. Zucker, A. Pinczuk, D. Chemla, A. Gossard, and W. Wiegmann, *Phys. Rev. B* **29**, 7065 (1984).

¹⁰F. Cerdeira, A. Pinczuk, and J. C. Bean, *Phys. Rev. B* **31**, 1202 (1985).

¹¹The subject of resonant Raman scattering in semiconductors has been recently reviewed by M. Cardona, in *Light Scattering in Solids II* (Springer, Heidelberg, 1982), pp. 19–198.

¹²P. Y. Yu and Y. P. Shen, *Phys. Rev. Lett.* **29**, 468 (1972).

¹³W. Dreybrodt, W. Richter, F. Cerdeira, and M. Cardona, *Phys. Status Solidi (b)* **60**, 145 (1973).

¹⁴W. Richter, R. Zeyher, and M. Cardona, *Phys. Rev. B* **18**, 4312 (1978).

¹⁵F. Cerdeira, A. Pinczuk, J. C. Bean, B. Batlogg, and B. A. Wilson, *Appl. Phys. Lett.* **45**, 1138 (1984).

¹⁶H. Shen and F. H. Pollak, *Appl. Phys. Lett.* **45**, 692 (1984).

¹⁷T. Tuomi, M. Cardona, and F. H. Pollak, *Phys. Status Solidi* **40**, 227 (1970).

¹⁸J. R. Chelikowsky and M. L. Cohen, *Phys. Rev. B* **14**, 556 (1976).